Catal Lett (2008) 124:133–138
DOI 10.1007/s10562-008-9440-6

Synthesis of Sulfated Silica-Doped Tin Oxides and Their High Activities in Transesterification

Yunchen Du · Sen Liu · Yanyan Ji · Yonglai Zhang · Shu Wei · Fujian Liu · Feng-Shou Xiao

Received: 21 September 2007 / Accepted: 11 February 2008 / Published online: 26 February 2008

Abstract A series of sulfated silica-doped tin oxides with large surface areas (113–188 m^2/g) have been successfully prepared from hydrothermal synthesis, followed by sulfation and calcination. These samples are characterized by XRD, FT-IR, TEM, nitrogen isotherms, and TG techniques, and obtained results indicate that the samples are composed of tetragonal nanocrystalline tin oxides and amorphous silica. Very interestingly, catalytic tests show that these sulfated silica-doped tin oxides are much more active than conventional sulfated tin oxides for transesterification of triacetin with methanol.

Keywords Sulfated tin oxides · Silica-doped · Tetragonal crystalline · Transesterification

1 Introduction

Biodiesel is a renewable fuel that can be produced by transesterifications from vegetable oils and short-chain alcohols in the presence of homogeneous catalysts such as sulfuric acid and sodium hydroxide [1–5]. However, these homogeneous catalysts usually have the disadvantages in separation and environmental pollution. Therefore, there is a great interest on developing catalytically active solids in transesterification [6–22]. Among them, basic solid catalysts exhibit excellent catalytic activities [7–14], but the interaction between CO_2 in air with these basic solid catalysts normally results in deactivation of these catalysts. In contrast, acidic solid catalysts which are also active for transesterification [16–23], are more chemically stable than basic solid catalysts. As typical acidic solids, sulfated zirconia and tungstated zirconia have been considered to be very effective catalysts for transesterification [20–23].

It is well known that sulfated tin oxides (SO_4^{2-}/SnO_2) is one of the candidates with strong acidity [24–26], giving higher catalytic activities in esterification and Friedel-Crafts acylation than sulfated zirconia [27, 28], but there are few reports concerning on its performance in transesterification. Conventionally, sulfated tin oxides prepared by precipitation method shows relatively small surface area, and one solution for this problem is to fabricate mesostructured sulfated tin oxides with enhanced catalytic activities [29–31]. Unfortunately, some of them exhibit poor thermal stability [29, 30].

Herein, we demonstrated a facile route to prepare sulfated silica-doped tin oxides from hydrothermal synthesis, followed by sulfation and calcination. Very interestingly, these samples have much higher BET surface areas (113–188 m^2/g) and better activities (84.8–91.1%) in transesterification of triacetin with methanol than conventional sulfated tin oxides (75 m^2/g, 77.5%).

2 Experimental Section

Sulfated silica-doped tin oxides was typically synthesized in the following: (1) 3.12 g of $SnCl_4 \cdot 5H_2O$ was dissolved in 50 mL of deionized water, followed by addition of a required amount of tetraethyl orthosilicate (TEOS), stirring for 10–12 h; (2) After stirring at 80 °C for 24 h, the mixture was transferred into a stainless steel autoclave for further crystallization at 100 °C for 24 h; (3) The solid

Y. Du · S. Liu · Y. Ji · Y. Zhang · S. Wei · F. Liu · F.-S. Xiao (✉)
State Key Laboratory of Inorganic Synthesis and Preparative Chemistry and College of Chemistry, Jilin University, Changchun 130012, China
e-mail: fsxiao@mail.jlu.edu.cn

products were collected by filtration, drying at 100 °C; (4) The solid sample (1 g) was immersed into 15 mL of 3 M H_2SO_4 at room temperature for 30 min, followed by filtration at room temperature, drying at 100 °C overnight, and calcination at 500 °C for 3 h, obtaining sulfated silica-doped tin oxides. A series of sulfated silica-doped tin oxides were denoted as sul-SnO_2(x), where x stands for the molar ratio of Si/Sn in the initial mixture.

For comparison, conventional sulfated tin oxides and zirconia denoted as ST and SZ, were prepared from published literature [32]. The calcination temperature for sulfated tin oxides and sulfated zirconia was 500 and 600 °C, respectively.

Powder X-ray diffraction (XRD) data were recorded on a Rigaku D/Max-2550 (40 kV, 200 mA), using nickel-filtered Cu $K\alpha$ radiation with wavelength of $\lambda = 1.5406$ Å. Nitrogen isotherms were obtained at −196 °C on a Micromeritics ASAP 2020. Samples were normally prepared for measurement by degassing at 150 °C. Pore size distribution was calculated using the Barrett–Joyner–Halenda (BJH) method. The molar ratio of Si/Sn in solid samples was determined by the results of inductively-coupled plasma analysis (ICP, Perkin-Elmer 3300DV). Transmission electron micrograph (TEM) was taken on a JEOL 3010 microscope operating at an accelerating voltage of 300 kV. Fourier-transform infrared (FT-IR) spectroscopy was performed on IFS 66V/S (Bruker) infrared spectrometer in the range 400–4000 cm^{-1} using KBr pellets, the samples were measured until a final pressure was 4×10^{-3} mbar. Thermogravimetric analysis (TG) was carried out using a Pyris Diamind TG with a heating rate of 10 K/min from room temperature to 1000 °C. The samples were mounted horizontally and purged with a synthetic airflow of 100 mL/min.

Catalytic transesterification of triacetin with methanol was performed in a 50 mL three-neck flask. The flask was kept in an oil bath with a temperature control of ±1 °C, and the reaction mixture was magnetically stirred. As a typical run of transesterification of triacetin with methanol, 100 mg of catalyst and 1.88 mL (10 mmol) of triacetin was added into the flask. After increasing the temperature to 60 °C, 3.64 mL (90 mmol) of methanol was added into the reactor. After reaction for 12 h, the products were analyzed by gas chromatography (Varian CP-3800) with a FID detector.

3 Rusults and Discussion

Figure 1 shows wide-angle XRD patterns of sulfated silica-doped tin oxides samples with various molar ratios of Si/Sn at 0–0.33. Obviously, all samples display five well-resolved peaks at ~26.8, 33.7, 37.8, 51.7, 65.0° assigned

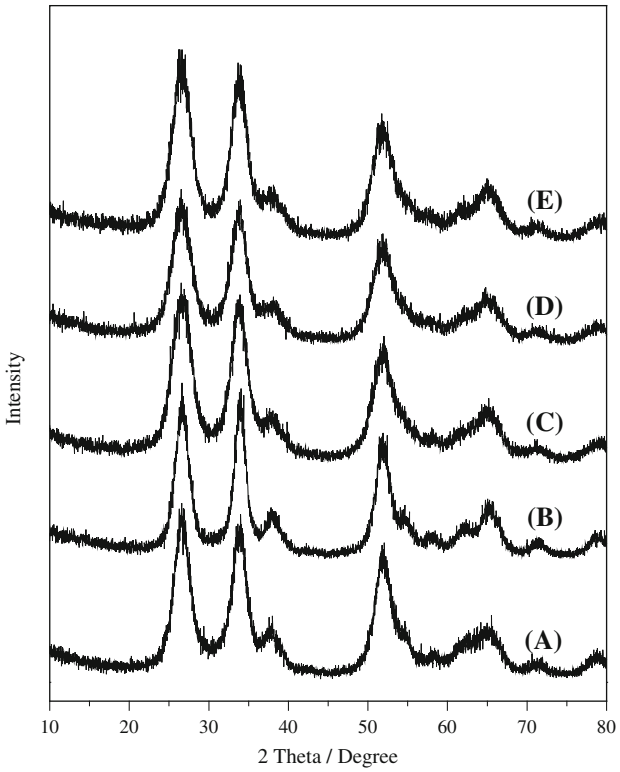

Fig. 1 The XRD patterns of (**A**) ST; (**B**) sul-SnO_2(0); (**C**) sul-SnO_2(0.20); (**D**) sul-SnO_2(0.25); (**E**) sul-SnO_2(0.33) in wide-angle region

to pure tetragonal phase of crystalline SnO_2, which is very important for the formation of strong acidic sites in sulfated tin oxides [28]. In contrast, there is no peak associated with SiO_2 in XRD pattern, suggesting that SiO_2 may be highly dispersed in sulfated tin oxides. Furthermore, ICP analysis shows that Si/Sn ratios are 0.062, 0.080, 0.114 for sul-SnO_2(0.20), sul-SnO_2(0.25), sul-SnO_2(0.33), respectively, indicating that only a partial of SiO_2 in the starting mixture was included in the final samples (Table 1).

Figure 2 shows FT-IR spectra of various samples. Notably, ST and sul-SnO_2(0) exhibit typical bands associated with sulfated tin oxides. However, sul-SnO_2(0.20), sul-SnO_2(0.25) and sul-SnO_2(0.33) show drastically increasing peaks around 960–1200 cm^{-1}, which can be assigned to the incorporation of SiO_2. These results further confirm the presence of silica species in these sulfated tin oxides.

As a typical example, Fig. 3 shows TEM images of sul-SnO_2(0.25). Low magnification image of the sample (Fig. 3a) clearly shows the presence of mesoporosity ranged at 2–7 nm, and high magnification image of the sample (Fig. 3b) demonstrates the sample is composed of nanocrystalline SnO_2 with sizes of 6–10 nm.

Figure 4 shows N_2 adsorption/desorption isotherms and pore size distribution of sulfated silica-doped tin oxides

Table 1 Textural parameters of various sulfated tin oxides[a]

Samples[b]	Si/Sn		BET (m^2/g)	Pore size (nm)	Pore volume (cm^3/g)	Sulfate content[c] (wt%)
	Initial solution	Final product				
ST	0	0	75	5.1	0.06	3.44
sul-SnO_2(0)	0	0	113	4.0	0.09	4.93
sul-SnO_2(0.20)	0.20	0.062	150	3.5	0.11	5.25
sul-SnO_2(0.25)	0.25	0.080	178	3.2	0.13	5.13
sul-SnO_2(0.33)	0.33	0.114	188	2.9	0.14	5.04

[a] Pore size distribution and pore volume determined from N_2 adsorption isotherms at −196 °C

[b] All samples were calcined at 500 °C for 3 h

[c] The contents of sulfate species were calculated from TG curves

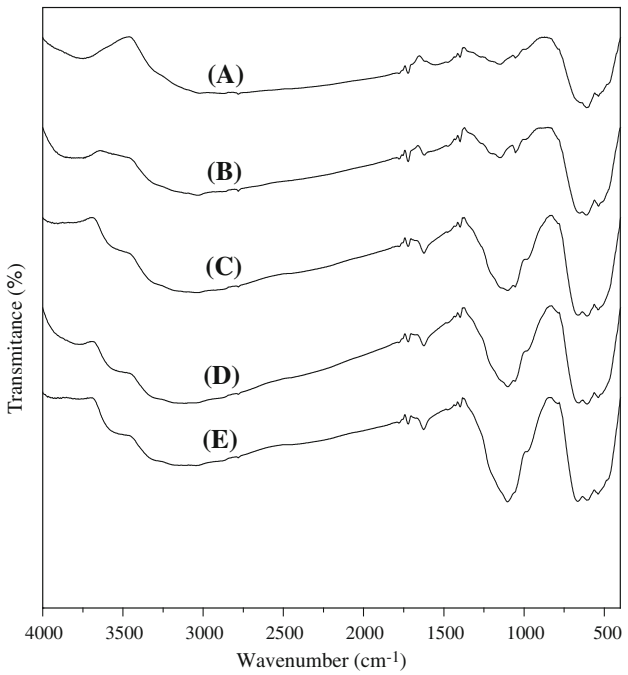

Fig. 2 FT-IR spectra of (**A**) ST; (**B**) sul-SnO_2(0); (**C**) sul-SnO_2(0.20); (**D**) sul-SnO_2(0.25); (**E**) sul-SnO_2(0.33)

samples with various molar ratios of Si/Sn at 0–0.33 and their textural parameters are presented in Table 1. Notably, after calcination at 500 °C for 3 h, all samples exhibit hysteresis loops at high relative pressure which is reasonably related to the capillary condensation associated with mesoporosity, indicating that mesoporosity in these samples is thermally stable. Furthermore, it is observed that all of the samples exhibit narrow pore size distribution, but their sizes are quite different from 2.9 to 4.0 nm. Normally, the mesoporosity in nanosized materials could be attributed to aggregation of nanoparticles each other, and larger pore sizes possibly indicate larger nanoparticles [33, 34]. Therefore, it is suggested that nanocrystals in ST and sul-SnO_2(0) may be larger than those in sul-SnO_2(x) (x = 0.20–0.33). These results also suggest that a little

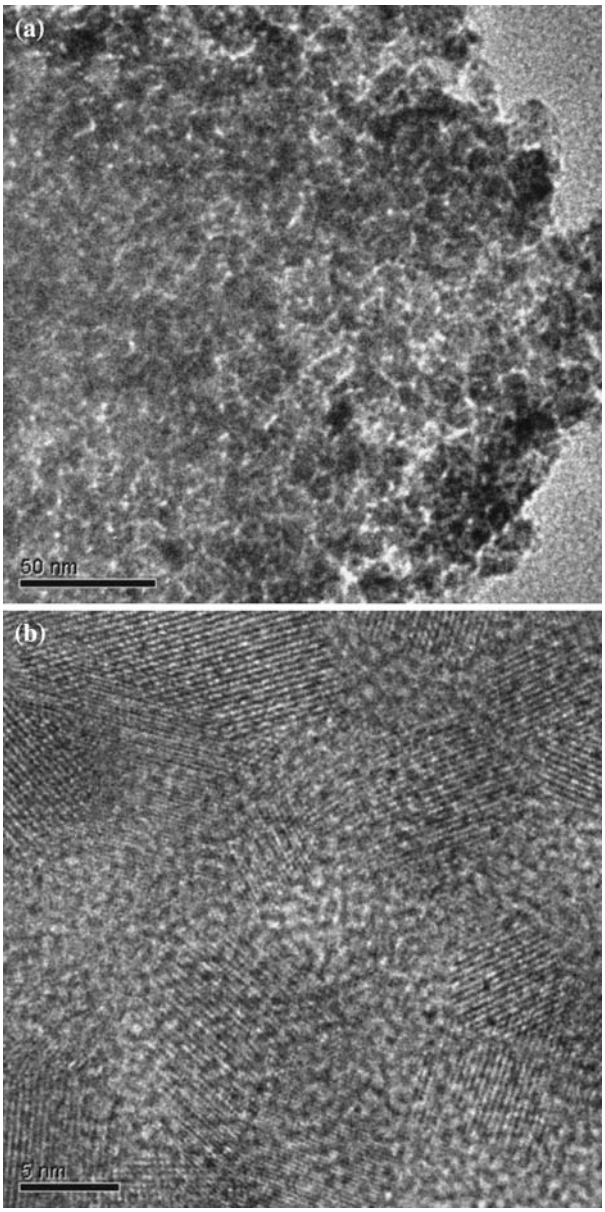

Fig. 3 TEM images of sul-SnO_2(0.25) with (**a**) low and (**b**) high magnification

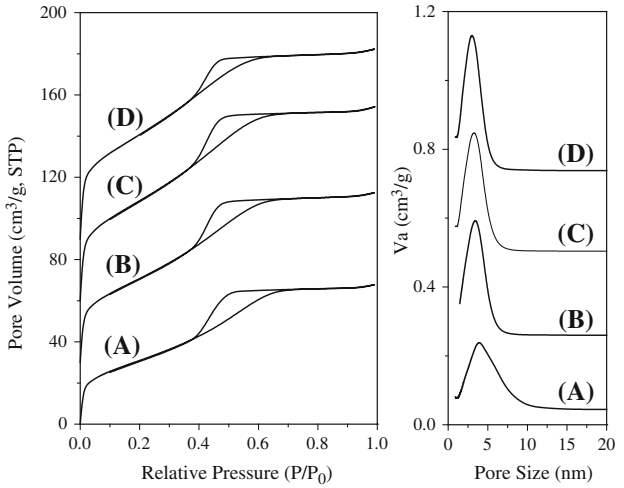

Fig. 4 N_2 adsorption/desorption isotherms and pore size distribution of (**A**) sul-SnO_2(0); (**B**) sul-SnO_2(0.20); (**C**) sul-SnO_2(0.25); (**D**) sul-SnO_2(0.33). Isotherms of (**B**), (**C**) and (**D**) have been offset by 30, 60 and 90 cm^3/g along the vertical axis for clarity, respectively

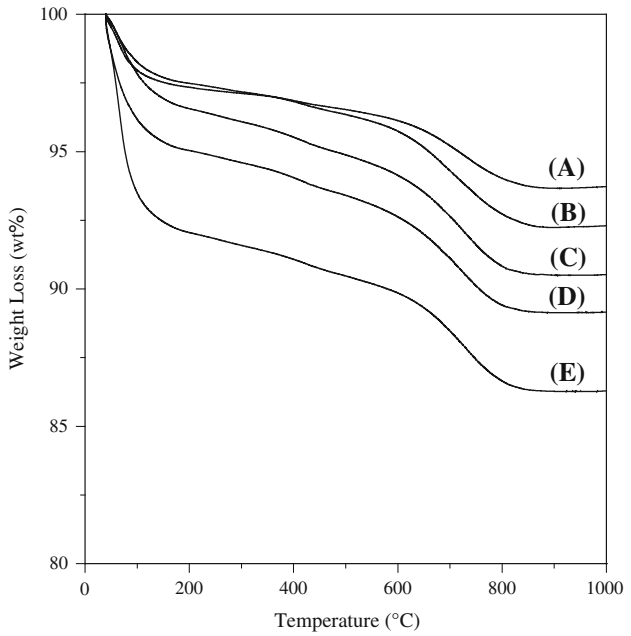

Fig. 5 TG curves of (**A**) ST; (**B**) sul-SnO_2(0); (**C**) sul-SnO_2(0.20); (**D**) sul-SnO_2(0.25); (**E**) sul-SnO_2(0.33)

amorphous SiO_2 has a good effect for the dispersion of SnO_2 nanocrystals during hydrothermal and thermal treatments.

It is worth noting surface area of various samples. Conventional sulfated SnO_2 (ST) shows BET surface area at 75 m^2/g. In contrast, sulfated SnO_2 synthesized from hydrothermal route (sul-SnO_2(0)) gives a larger surface area (113 m^2/g), suggesting that crystal sizes of sul-SnO_2(0) sample may be much smaller than those of ST sample [33]. When a little of amorphous SiO_2 is mixed with SnO_2 under hydrothermal condition, BET surface

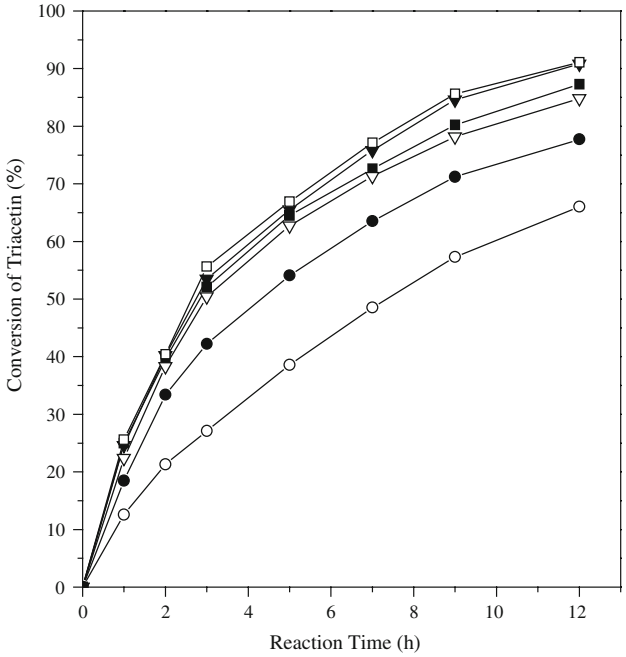

Fig. 6 Dependences of triacetin conversion on reaction time over various catalysts. (○) SZ; (●) ST; (▽) sul-SnO_2(0); (□) sul-SnO_2(0.20); (▼) sul-SnO_2(0.25); (■) sul-SnO_2(0.33)

areas of the samples (sul-SnO_2(x), x = 0.20–0.33) are increased up to 150–188 m^2/g (Table 1).

Figure 5 shows the TG curves of various samples. All samples give two weight-loss steps: the first step below 200 °C is due to the desorption of water; the second step between 500 and 900 °C is attributed to the decomposition of sulfate species on the sample [35]. Based on the curves, the amount of sulfate species on the surface of sul-SnO_2(x) (x = 0–0.33) are estimated between 4.93 and 5.25 wt%, which is much higher than that on the surface of ST (3.44%) (Table 1). Generally, the higher sulfate species may be helpful in catalysis for sulfated metal oxides [28, 31, 34, 36, 37].

Figure 6 shows the dependence of catalytic activities on reaction time in catalytic transesterification of triacetin with methanol over various samples. Notably, all samples exhibit good catalytic properties in the transesterification. For example, SZ gives conversion of triacetin at 66.0% after 12 h, in good agreement with literature [14], but ST exhibits higher catalytic activity (77.5%) and better selectivity for glycerol (50.4%) (Table 2). Interestingly, sul-SnO_2(x) samples (x = 0–0.33) exhibit much better activities and selectivities than ST (Table 2), which may be reasonably related to the differences in their surface area (Fig. 4) and sulfate species content (Fig. 5, Table 1). For example, sul-SnO_2(0) give conversion at 84.8% and selectivity of glycerol at 60.9%, which are obviously higher than those of ST (conversion at 77.5% and selectivity for 50.4%). Furthermore, it is observed that sample

Table 2 Transesterification of triacetin with methanol over various catalysts[a]

Catalysts	Conversion (%)	Selectivity		
		Glycerol (%)	Monoacetin (%)	Diacetin (%)
SZ	66.0	29.8	34.5	35.7
ST	77.5	50.4	29.3	20.3
sul-SnO_2(0)	84.8	60.9	27.0	12.1
sul-SnO_2(0.20)	91.1	68.4	24.8	6.8
sul-SnO_2(0.25)	90.8	66.4	25.8	7.8
sul-SnO_2(0.33)	87.3	66.5	24.5	9.0

[a] Reaction conditions: 10 mmol of triacetin, 90 mmol of methanol, 100 mg of catalyst, reaction temperature at 60 °C, reaction time 12 h. The conversion was calculated from triacetin

activities and selectivities increase with the molar ratios of Si/Sn in the sul-SnO_2(x) samples from 0 to 0.20. However, the activities and selectivities decrease with the ratio of Si/Sn from 0.20 to 0.33, and this phenomenon is mainly due to diminution of sulfated tin oxides sites in the samples (Table 1).

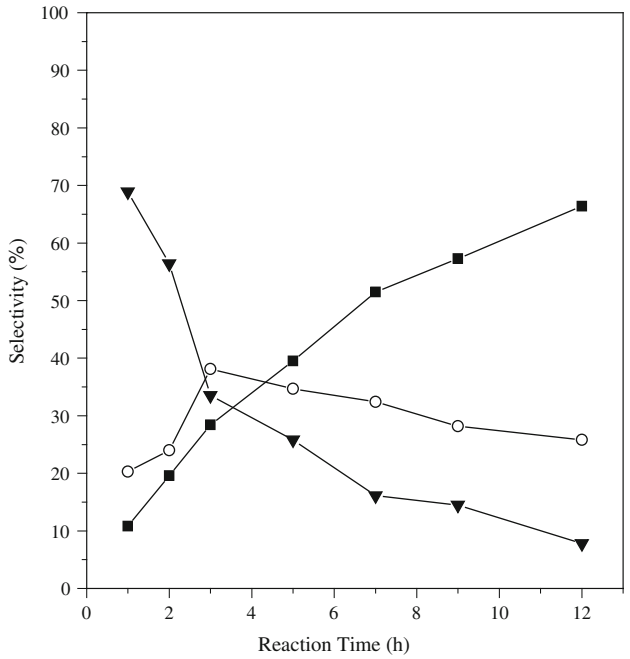

Fig. 7 Dependences of products distribution on reaction time over sul-SnO_2(0.25) catalyst. (■) Glycerol; (○) Monoacetin; (▼) Diacetin

As a typical sample, Fig. 7 shows the product selectivities for glycerol, monoacetin, and diacetin in transesterification of triacetin with methanol over sul-SnO_2(0.25) at various reaction time. When the reaction time at 1 h, diacetin is a main product (68.9%), and monoacetin (20.3%) and glycerol (10.8%) are limited. When the reaction time is increased to 3 h, monoacetin gives the highest selectivity. When the reaction time is increased up to 12 h, glycerol is dominant (66.4%).

For testing their heterogeneous nature, the recycles of catalysts have been carried out. Notably, after one recycle, all of catalysts show decrescent surface area and enhancive pore volume and pore size (Table 3), which indicates that the nanoparticles in these samples have been partially aggregated during the reaction recycle. Correspondingly, these catalysts give relatively low activities, compared with the fresh catalysts. Interestingly, compared with sul-SnO_2(0), sul-SnO_2(x) samples (x = 0.20–0.33) still exhibit relatively high catalytic activities, suggesting that the presences of SiO_2 in sul-SnO_2(x) is very helpful for increasing catalyst life. Even after three recycles, sul-SnO_2(0.20) still gives higher conversion (78.5%) than sul-SnO_2(0) recycled for one time (71.1%). These results indicate that sul-SnO_2(x) samples could be used as heterogeneous catalysts for transesterification of triacetin with methanol.

Table 3 Textural parameters and catalytic properties of various catalysts after one recycle[a]

Catalysts	BET (m^2/g)	Pore size (nm)	Pore volume (cm^3/g)	Conversion (%)	Selectivity		
					Glycerol (%)	Monoacetin (%)	Diacetin (%)
ST	52	6.4	0.09	70.2	48.5	30.2	21.3
sul-SnO_2(0)	64	6.0	0.12	71.1	51.1	30.5	18.4
sul-SnO_2(0.20)	119	3.6	0.15	84.3	61.3	25.0	13.7
sul-SnO_2(0.20)[b]	106	3.6	0.13	78.5	56.4	27.4	16.2
sul-SnO_2(0.25)	143	3.5	0.17	81.8	59.2	26.4	14.4
sul-SnO_2(0.33)	160	3.3	0.18	78.7	56.3	27.6	16.1

[a] The catalysts were recycled by filtrating at room temperature, treating in H_2SO_4 solution (0.5 M), and calcination at 500 °C for 1 h

[b] The conversion was obtained after three recycles

4 Conclusions

In summary, a series of sulfated silica-doped tin oxides samples have been successfully prepared through hydrothermal synthesis, followed by sulfation and calcination. These samples show higher BET surface areas and sulfate species, compared with conventional sulfated SnO_2. Very importantly, these samples exhibit much higher catalytic activities than conventional sulfated SnO_2 and ZrO_2, which would be potentially important for the production of biodiesel in the future.

Acknowledgments This work was supported by the National Natural Science Foundation of China (20573044 and 20773049) and State Basic Research Project of China (2003CB615802).

References

1. Ma F, Hanna MA (1999) Bioresour Technol 70:1
2. Otera J (1993) J Chem Rev 93:1449
3. Davies B, Jeffreys GV (1973) Trans Inst Chem Eng 51:271
4. Freedman B, Butterfield RO, Pryde EH (1986) J Am Oil Chem 63:1375
5. Schmidt J, Reusch D, Elgeti K, Schomäcker R (1999) Chem Ing Tech 71:704
6. Corma A, Iborra S, Velty A (2007) Chem Rev 107:2411
7. Hoelderich WF (2000) Catal Today 62:115
8. Leclercq E, Finiels A, Moreau C (2001) J Am Oil Chem 78:1161
9. Xie WL, Peng H, Chen LG (2006) Appl Catal A 300:67
10. Cantrell DG, Gillie LJ, Lee AF, Wilson K (2005) Appl Catal A 287:183
11. Corma A, Abd Hamid SB, Iborra S, Velty A (2005) J Catal 234:340
12. Wang H, Wang MH, Zhao N, Wei W, Sun YH (2005) Catal Lett 105:253
13. Dossin TF, Reyniers MF, Marin GB (2006) Appl Catal B 62:35
14. Lopez DE, Goodwin JG, Bruce DA, Lotero E (2005) Appl Catal A 295:97
15. Sricastava R, Srinivas D, Ratnasamy P (2006) J Catal 241:34
16. Lotero E, Liu Y, Lopez DE, Suwannakarn K, Bruce DA, Goodwin JG Jr (2005) Ind Eng Chem Res 44:5353
17. Mbaraka IK, McGuire KJ, Shanks BH (2006) Ind Eng Chem Res 45:3022
18. Lopez DE, Goodwin JG, Bruce DA (2007) J Catal 245:381
19. Chai F, Cao F, Zhai F, Chen Y, Wang XH, Su Z (2007) Adv Synth Catal 349:1057
20. Furuta S, Matsuhashi H, Arata K (2004) Catal Commun 5:721
21. Shamshuddin SZM (2005) Synlett 16(2):361
22. Shamshuddin SZM, Nagaraju N (2006) Catal Commun 7:593
23. Lopez DE, Suwannakarn K, Bruce DA, Goodwin JG (2007) J Catal 247:43
24. Matsuhashi H, Hino M, Arata K (1998) Chem Lett 1027
25. Matsuhashi H, Hino M, Arata K (1990) Appl Catal 59:205
26. Wang GW, Hattori M, Tanabe K (1983) Chem Lett 277
27. Matsuhashi H, Miyazaki H, KawaMura Y, Nakamura H, Arata K (2001) Chem Mater 13:3038
28. Furata S, Matsuhashi H, Arata K (2004) Appl Catal A 269:187
29. Scott RWJ, Mamak M, Wong KK, Coombs N, Ozin GA (2003) J Mater Chem 13:1046
30. Qi L, Ma J, Cheng H, Zhao Z (1998) Langmuir 14:2579
31. Du YC, Liu S, Zhang Y, Yin C, Di Y, Xiao F-S (2006) Catal Lett 108:155
32. Arata K (1996) Appl Catal A 146:3
33. Fujihara S, Maeda T, Ohgi H, Hosono E, Imai H, Kim S-H (2004) Langmuir 20:6476
34. Sun Y, Ma S, Du Y, Yuan L, Wang S, Yang J, Deng F, Xiao F-S (2005) J Phys Chem B 109:2567
35. Guierrez-Baez R, Toledo-Antonio JA, Cortes-Jacome MA, Sebastian PJ, Vazquez A (2004) Langmuir 20:4265
36. Corma A (1995) Chem Rev 95:559
37. Sun Y, Yuan L, Wang W, Chen C-L, Xiao F-S (2003) Catal Lett 87:57